

RSC Advances



This is an *Accepted Manuscript*, which has been through the Royal Society of Chemistry peer review process and has been accepted for publication.

Accepted Manuscripts are published online shortly after acceptance, before technical editing, formatting and proof reading. Using this free service, authors can make their results available to the community, in citable form, before we publish the edited article. This *Accepted Manuscript* will be replaced by the edited, formatted and paginated article as soon as this is available.

You can find more information about *Accepted Manuscripts* in the [Information for Authors](#).

Please note that technical editing may introduce minor changes to the text and/or graphics, which may alter content. The journal's standard [Terms & Conditions](#) and the [Ethical guidelines](#) still apply. In no event shall the Royal Society of Chemistry be held responsible for any errors or omissions in this *Accepted Manuscript* or any consequences arising from the use of any information it contains.

COMMUNICATION

Efficient Energy Transfer in Eu-doped ZnO on diamond film

Cite this: DOI: 10.1039/x0xx00000x

Qi Yu,*^a Taotao Ai,^a Liyun Jiang,^b Yingtang Zhang,^a Chuang Li^aand Xinqiang Yuan^aReceived 00th August 2014,
Accepted 00th August 2014

DOI: 10.1039/x0xx00000x

www.rsc.org/

Eu-zinc oxide (ZnO) has been fabricated on p-diamond substrate by hydrothermal technique. Efficient Eu-ZnO/diamond visible light emission is observed in the electroluminescence process. The mechanism for the energy transfer behavior and the emissions is discussed.

Semiconductors doped with rare earth (RE) elements have attracted much attention in recent years due to their novel optical properties and promising applications in many fields, such as fiber amplifiers, light emitting devices and fluorescent lamps.¹⁻⁴ In most of these applications, efficient energy transfer from host to the RE³⁺ is desired. ZnO with a bandgap of 3.37 eV and a bound exciton energy of 60 meV is also an important semiconductor for which UV and visible emissions are widely reported.⁵ Unfortunately, the work of harvesting intense Eu³⁺ emission from ZnO films, ceramics, and powders remains disappointing because of the strong quenching effect of the wide-band, self-activated, green or yellow emissions and the higher energy-level position of Eu³⁺ relative to the bottom conduction band (CB).⁶ It has been established that direct ZnO→Eu³⁺ energy transfer seems physically impossible, as the radiative and nonradiative decay of excitons in ZnO are >10² times faster than the energy-transfer rate of RE³⁺. Fortunately, energy transfer can be facilitated by the presence of intrinsic or extrinsic defects as energy trap centers in various systems, such as ZnO/diamond,⁷ which suggests that the introduction of an appropriate trap center is crucial for efficient ZnO→Eu³⁺ energy transfer. Several groups have reported that defects, either intrinsic or extrinsic, can serve as the energy trapping centers to facilitate energy transfer and relevant light emission. Park et al. indicated that extrinsic defects like chlorine impurities can assist the red emission in Eu³⁺-doped ZnO.⁸ Wang et al. reported the surface defects may act to help the process of energy transfer from ZnO to Eu³⁺ ions.⁹ Zeng et al. indicated that in Eu-doped ZnO microspheres Eu²⁺ ions act as the trapping centers and transfer energy to Eu³⁺ ions, leading to the emission.¹⁰

In this work, nanostructural Eu doped n-ZnO on p-type diamond has been fabricated to research the current-voltage (*I-V*), electroluminescence (EL) and photoluminescence (PL) properties. For the first time, efficient Eu-ZnO/diamond visible light emission was observed. The Eu-ZnO/diamond has been realized with good

rectifying behavior. By first-principles calculation, it is demonstrated that the doped Eu atoms are favorable to the octahedral interstice in ZnO lattice.

The polycrystalline diamond film is deposited on Si wafer by hot filament CVD system.¹¹ Boron source of diborane or trimethylborate was additionally introduced to the reaction gases of methane/hydrogen (CH₄/H₂). Before the hydrothermal process, a ZnO seed layer was deposited by radio frequency (at 13.56 MHz) magnetron sputtering process. For the hydrothermal growth, the aqueous solution of zinc acetate dihydrate and hexamethylenetetramine aqueous solution of equal concentration (0.01 M) were mixed together and kept under mild magnetic stirring for 30 min, and then the europium nitrate (Eu(NO₃))₃ was added into the precursor solution with different concentrations. The autoclaves were sealed and heated to a constant temperature of 95 °C for 6 h. The products of ZnO/diamond were thoroughly washed with distilled water to remove the residual salts before dried naturally in air.

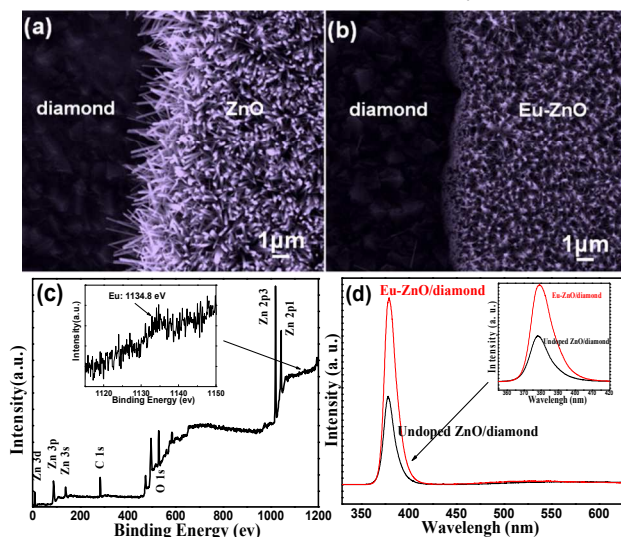


Fig. 1. SEM images of (a) undoped and (b) Eu-doped ZnO grown on p-typed diamond substrates. (c) XPS spectrum of sample B, and (d) PL spectra of samples A and B.

ARTICLE

The morphologies and composition of the sample was characterized by means of scanning electron microscopy (SEM, by JEOL JXA-8200 electron probe micro-analyzer), X-ray diffraction (XRD, by Rigaku D/MAX-RA with Cu K α radiation), and X-ray photo electron spectroscopy (XPS, by VG Escalab MK). The photoluminescence (PL) measurements were carried out excited by He-Cd laser (wavelength 325 nm) at room temperature, and the current-voltage (I - V) measurements were performed by a Keithley 2400 sourcemeeter.

Figs. 1a and 1b are the SEM images of ZnO (sample A) and Eu-ZnO (sample B), respectively. For sample A, the highly (001)-oriented ZnO NRs with a hexagonal top facet were uniformly grown on the diamond film. The average diameter of the ZnO is about 150 nm for sample A. For sample B, the average diameter of the ZnO nanorods is about 80 nm, and the top of rods gathers. The thickness of the samples are different, sample A is thicker than sample B. In the XPS spectrum of the Eu-ZnO of sample B (Fig. 1c), the peak appears at 1134.8 eV meaning the existence of Eu chemically bonded to oxygen (O). The atomic concentration of Eu in ZnO calculated is of 0.67 at. %. The room temperature PL spectra of samples A and B excited by He-Cd laser (wavelength 325 nm) are shown in Fig. 1d. The strong peak near band edge UV emission at about 378 nm. Gu et al. have reported that the peak near band edge UV emission of ZnO originates from the recombination of free excitons.¹² After Eu doping, the UV peak has a light red left, which is attributed to the size of nanostructures, as well as increase in Zn interstitials near the surface.

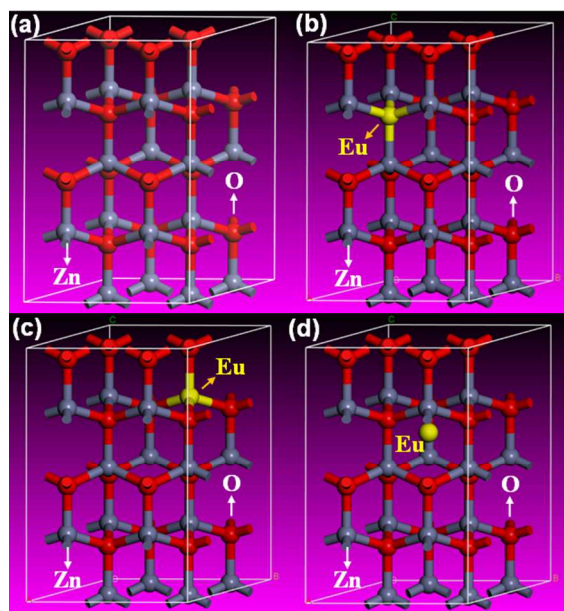


Fig. 2. Calculated supercell structures of (a) pure ZnO, with (b) a substituted Eu atom of oxygen, (c) a substituted Eu atom of zinc, and (d) an interstitial Eu atom in ZnO lattice.

Fig. 2 shows the calculated structures of ZnO with/without Eu doping. The optimizations are performed by first-principles calculations within the generalized gradient approximation as implemented in the CASTEP.¹³ The Norm-conserving pseudopotentials are used in conjunction with plane-wave basis sets of energy of 600 eV with $2 \times 2 \times 2$ supercell model. In the supercell, 32 Zn and 32 O atoms are selected with one Eu atom. There are three possible sites for boron atoms incorporated in ZnO lattice, i.e., in the octahedral interstice, substitute the O or Zn site. For comparison, the calculated results of undoped ZnO are illustrated in

Fig. 2a. Figs. 2(b)–2(d) present the optimized configurations of one Eu atom incorporated into the ZnO supercell (i) substituting O (Fig. 2b) and (ii) Zn position (Fig. 2c), and (iii) as an interstitial atom in ZnO (Fig. 2d). The ZnO lattices are distorted and obviously changes in bond length after boron doping. In addition, the formation energies (FE) of the structural optimization for the interstitial and substituted types of B atom in ZnO lattice are calculated, following the equations (1) and (2), respectively:¹⁴

$$FE = (E_{\text{cal}} - 16E_{\text{Zn}} - 16E_{\text{O}} - E_{\text{Eu}}) / 33 \quad (1)$$

$$FE = (E_{\text{cal}} - 15E_{\text{ZnO}} - 16E_{\text{O/Zn}} - E_{\text{Eu}}) / 32 \quad (2)$$

Where E_{cal} are the total energies of the calculated ZnO supercells, E_{ZnO} and E_{Eu} are the chemical potential of Zn (or O) and Eu per unit cell. After structural optimization, there is a decrease trend of FE for the three cases, i.e., (i) > (ii) > (iii), suggesting that the case of octahedral interstice (iii) is more energetically favorable rather than that of (i) and (ii). Taking into the calculations, it is reasonably proposed that the Eu atoms in ZnO lattice are favorable localizing in the octahedral interstice.

The I - V characteristics of Eu-doped (marked by red) and undoped (marked by black) samples are illustrated in Fig. 3a. Inset is the schematic diagram of the ZnO/diamond heterojunction diode. A transparent conductive indium-tin-oxide (ITO) glass is pressed on the top of ZnO as the cathode. The silver (Ag) slurry is used as the ohmic contacts to ITO and diamond. Comparing to the Eu-doped ZnO/diamond, there isn't obvious heterojunction for the undoped sample, suggesting that the Eu-doped ZnO/diamond-based device has relatively higher I - V performance. The turn-on voltage of the Eu-doped ZnO/diamond is 2.0 V. When the bias is applied to 4 V, the current reaches to 1.0 mA, meanwhile, the reverse leakage current is ~ 0.1 mA at -4 V.

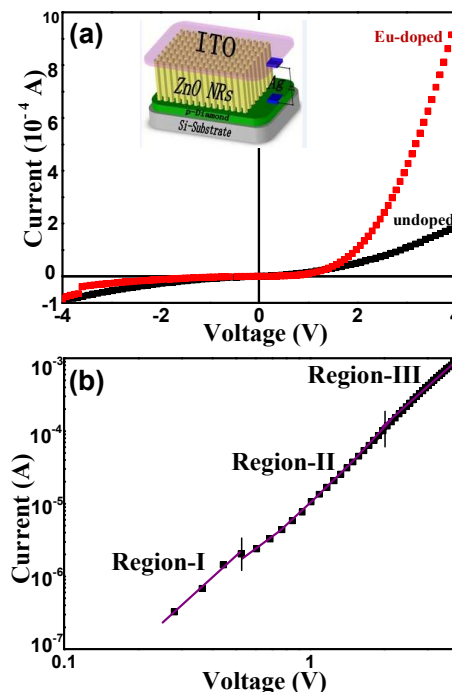


Fig. 3. I - V characteristics of Eu-doped and undoped ZnO/diamond heterojunction (a). Inset is the schematic diagram of device structure. (b) log-log I - V curve of the device.

Fig. 3b shows the log-log I - V curve of the device. The plot exhibits three distinct regions depending on the junction bias

voltage. At low forward voltages in region I ($<0.52\text{V}$), the power law of $I \sim V^{1.6}$ is observed. Reddy et al. have reported that the exponent approach to 1 means the improvement of Ohmic behavior.¹⁵ The exponent of 1.6 greater than 1 can be attributed to the presence of defect states in the interfaces, carrier injection has been significantly improved and the enlargement of the exponent can also be attributed to the more thermally excited carriers appearing.¹⁶ For region II ($0.52\text{V} < V < 2.12\text{V}$), the current follows an exponential relation $I \sim \exp(\alpha V)$, and this relation is usually proposed for the wide band gap p-n diodes related to a recombination-tunneling mechanism. In region III beyond 2.12V , the current conduction is attributed to the space-charge-limited current (SCLC) generally observed in wide band gap semiconductors.¹⁷ In the present cases, the SCLC is mainly for a single carrier (hole) injection because the concentration of holes is larger than the electrons. Since the band gap energy (electron affinity) of diamond is 5.47eV (0.50eV), which is larger (smaller) than the data of ZnO (band gap energy: 3.37eV , electronaffinity: 4.35eV), when the n-ZnO and p-diamond are joined, the bending of the conduction band is much higher than that of the valenceband. The higher barrier in the conduction band prevents the movement of electrons. Therefore, the conductive property of this heterojunction is determined mainly by the holes in the valence band.

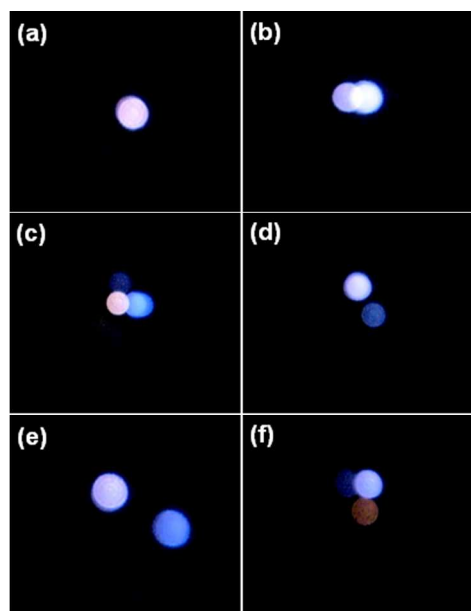


Fig. 4. Visible light emission of Eu ZnO/diamond in the electroluminescence process

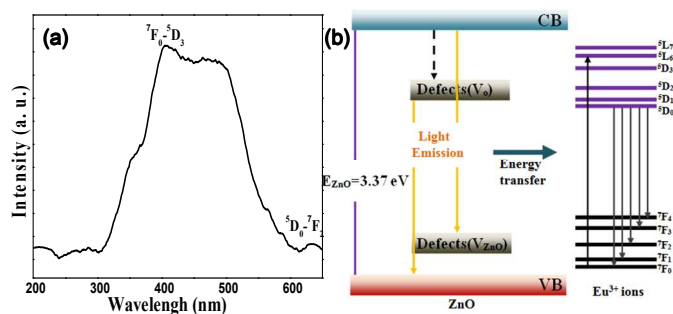


Fig. 5. (a) Emission spectrum of Eu-doped ZnO/diamond. (b) Schematic diagram illustrating the mechanism of the energy transfer behavior and the emissions of ZnO and Eu^{3+} ions.

The electroluminescence property of Eu-ZnO/diamond is investigated in Fig. 4(a)-(f). We can see visible light emission of Eu-ZnO/diamond as time goes by. Visible light can be observed during the process. The emission spectrum of electroluminescent device has been carried out at 200nm at room temperature (Fig. 5a). Peaks centered at 411nm should be ascribed to the direct excitation of the Eu^{3+} ions from the ground state ${}^7\text{F}_0$ to excited level ${}^5\text{D}_3$. In europium, the ${}^5\text{D}_0 \rightarrow {}^7\text{F}_1$ (613nm) is a hypersensitive forced electric-dipole transition being allowed only at low symmetries with no inversion center.¹⁰ A mechanism to account for the energy transfer behavior and the emissions of ZnO and Eu^{3+} ions is summarized in Fig. 5b. The excitation energy absorbed by ZnO promotes the electrons from the valence band (VB) to the conduction band. The electrons are then trapped by the defect states through the radiative decay process. The recombination of the electrons in the defect states with the holes in the VB results in the ZnO UV emission. Alternatively, for the sample doped with Eu^{3+} , a part of the recombination energy is transferred to the Eu^{3+} ions to promote their electrons from the ground state to the excited ones, which generates the Eu^{3+} emissions through the subsequent radiative relaxations. Zeng et al. have reported that the charge-carrier and energy-transfer determine the intensity of Eu^{3+} emission,¹⁰ and in our experiment, there's mainly energy transfer from ZnO to Eu^{3+} ions. Meanwhile, the Eu^{3+} ions can absorb the energy transferred from the defect emission of ZnO host, resonantly exciting the ${}^7\text{F}_J \rightarrow {}^5\text{D}_0$ transition.¹⁸ Then the electrons transfer from ${}^5\text{D}_0$ state to ${}^7\text{F}_J$ ($J = 0-4$) state of Eu^{3+} ions, resulting in the light emission. Note that there are no Eu^{3+} f-f bands in the emission spectra. Following bandgap excitation, the carriers relax to the band edge of the CB and VB, where they are rapidly trapped at the defects or undergo subsequent band edge, radiative emission. Wang et al. reported that by means of a resonant energy transfer process, the trapped carriers at the oxygen vacancies could transfer their energy to the Eu^{3+} subsystem. As a final step of the energetic process, Eu^{3+} ions go through the radiative transition from D to F, giving out the emission.¹⁹

Conclusions

In summary, nanostructural Eu doped n-ZnO has been fabricated on p-type diamond by hydrothermal method. It is demonstrated that the doped Eu atoms are favorable to the octahedral interstice in ZnO lattice by first-principles calculation. The ZnO/p-diamond heterojunction has been realized with good rectifying behavior. Efficient Eu-ZnO/diamond light emission was observed in the electroluminescence process. The results demonstrated that Eu doped ZnO nanstructure has a promising application for electronic devices.

Acknowledgements

This work is supported by the National Natural Science Foundation of China (Grant No. 51201094), the Natural Science Foundation of Shaanxi Province, China (Grant No. 2012JM6018) and the Science and Technology Program for Young Technology New Star of Shaanxi Province, China (Grant No. 2014KJXX-75). Scientific Research Startup Program for Introduced Talents of Shaanxi University of Technology, China (Grant No. SLGQD14-11). Scientific Research Startup Program for Introduced Talents of Shaanxi University of Technology, China (Grant No. SLGQD14-06). CASTEP software of Dr. Ping Peng research group in Hunan University.

Notes and references

ARTICLE

^a School of Materials Science and Engineering, Shaanxi University of Technology, Hanzhong 723001, P. R.China.

E-mail address: kukukoko2004@163.com

^b School of Physics and Telecommunication Engineering, Shaanxi University of Technology, Hanzhong 723001, P. R.China

1. J. Bang, H. Yang and P. H. Holloway, *J. Chem. Phys.*, 2005, **123**, 084709.
2. S. M. Ahmed, P. Szymanski, L. M. El-Nadi and M. A. El-Sayed, *ACS. Appl. Mater. Interfaces*, 2014, **6**, 1765.
3. Y. Xie, P. Joshi, S. B. Darling, Q. L. Chen, T. Zhang, D. Galipeau and Qiquan Qiao, *J. Phys. Chem. C*, 2010, **114**, 17880.
4. R. Shimada, B. Urban, M. Sharma, A. Singh, V. Avrutin, H. Morkoc and A. Neogi, *Opt. Mater. Express*, 2012, **2**, 526.
5. H. Yan, J. Johnson, M. Law, R. He, K. Knutsen, J. R. McKinney, J. Pham, R. Saykally and P. Yang, *Adv. Mater.*, 2003, **15**, 1907.
6. P. Dorenbos and E. Vander Kolk, *Appl. Phys. Lett.*, 2006, **89**, 061122.
7. Q. Yu, H. D. Li, Q. L. Wang, S. H. Cheng, L. Y. Jiang, Y. T. Zhang, T. T. Ai and C. S. Guo, *Mater. Lett.*, 2014, **128**, 284.
8. Y. K. Park, J. L. Han, M. G. Kwak, H. Yang, S. H. Ju and W. S. Cho, *Appl. Phys. Lett.*, 1998, **72**, 668.
9. M. Wang, C. Huang, Z. Huang, W. Guo, J. Huang, H. He, H. Wang, Y. Cao, Q. Liu and J. Liang, *Opt. Mater.*, 2009, **31**, 1502.
10. X.Y. Zeng, J.L. Yuan, Z.Y. Wang, L.D. Zhang, *Adv. Mater.*, 2007, **19**, 4510.
11. H. D. Li, G. T. Zou, Q. L. Wang, S. H. Cheng, B. Li and J. N. Lv, *Chin. Phys. Lett.*, 2008, **25**, 1803.
12. X. Q. Gu, L. P. Zhu, Z. Z. Ye, H. P. He, Y. Z. Zhang, F. Huang, M. X. Qiu, Y. J. Zeng, F. Liu and W. Jaeger, *Appl. Phys. Lett.*, 2007, **91**, 022103.
13. J. Bang, H. Yang and P. H. Holloway, *J. Chem. Phys.*, 2005, **123**, 084709.
14. L. Chen, *Journal of Changsha Aeronautical Vocational and Technical College*, 2008, **8**, 43.
15. N. K. Reddy, Q. Ahsanulhaq, J. H. Kim and Y. B. Hahn, *Appl. Phys. Lett.*, 2008, **92**, 043127.
16. D. D. Shang, H. D. Li, S. H. Cheng, Q. L. Wang and Q. Yu, *J. Appl. Phys.*, 2012, **112**, 036101.
17. R. Ghosh and D. Basak, *Appl. Phys. Lett.*, 2007, **90**, 2431061.
18. Y. L. Yu, Y. S. Wang, D. Q. Chen, P. Huang, E. Ma, and F. Bao, *Nanotechnology*, 2008, **19**, 055711.
19. D. D. Wang, G. Z. Xing, M. Gao, L. L. Yang, J. H. Yang and T. Wu, *J. Phys. Chem C*, 2011, **115**, 22729.